Magnetically modified electrocatalysts for oxygen evolution reaction in proton exchange membrane (PEM) water electrolyzers

Kaya, Mehmet; Demir, Nesrin; Rees, Neil; El-Kharouf, Ahmad

DOI:
10.1016/j.ijhydene.2021.03.203

Document Version
Peer reviewed version

Citation for published version (Harvard):
Kaya, M, Demir, N, Rees, N & El-Kharouf, A 2021, 'Magnetically modified electrocatalysts for oxygen evolution reaction in proton exchange membrane (PEM) water electrolyzers', *International Journal of Hydrogen Energy*, vol. 46, no. 40, pp. 20825-20834. https://doi.org/10.1016/j.ijhydene.2021.03.203

Magnetically Modified Electrocatalysts for Oxygen Evolution Reaction in Proton Exchange Membrane (PEM) Water Electrolyzers

Mehmet Fatih Kaya [1,2], Nesrin Demir [1*], Neil V. Rees [2], Ahmad El-Kharouf [2]

[1]Erciyes University, Engineering Faculty, Energy Systems Engineering Department, Heat Engineering Division, 38039, Kayseri, Turkey

[2]Centre for Fuel Cell & Hydrogen Research, School of Chemical Engineering, University of Birmingham, Birmingham, UK

* Corresponding author. Tel.: +903522076666-32330; Fax: +903524375784.

E-mail address: nkayatas@erciyes.edu.tr

ABSTRACT

Green hydrogen production can only be realized via water electrolysis using renewable energy sources. Proton exchange membrane water electrolyzers have been demonstrated as the technology of choice for mass production of green hydrogen due to their scalability and potential high efficiency. However, the technology is still relatively expensive due to the catalyst materials cost and operational limitations due to mass transfer and activation polarizations. During the oxygen evolution reaction, oxygen bubbles stick to the electrode surface and this causes a low reaction rate and high mass transfer losses. In this study, the commonly used electrocatalyst for oxygen evolution reactions; IrO_2, is modified by introducing magnetic Fe_3O_4 to achieve greater bubble separation at the anode during operation. The prepared composite catalysts were characterized using Scanning Electron Microscope, Energy Dispersive X-Ray Analysis, X-Ray Powder Diffraction, X-ray photoelectron spectroscopy and Brunauer–Emmett–Teller characterization methods. The modified composite electrocatalyst samples are magnetized to investigate the magnetic field effect on oxygen evolution reaction performance in proton exchange membrane water electrolyzers. 90% IrO_2 - 10% Fe_3O_4 and 80% IrO_2 - 20% Fe_3O_4 samples are tested via linear sweep voltammetry both ex-situ and in-situ in a proton exchange membrane water electrolyzer single cell. According to the linear sweep voltammetry tests, the magnetization of the 80% IrO_2 - 20% Fe_3O_4 sample resulted in 15% increase in the maximum current density. Moreover, the single cell electrolyzer test showed a four-fold increase in current density by employing the magnetized 80% IrO_2 - 20% Fe_3O_4 catalyst.

Keywords: Electrocatalysts, Kelvin Force, Lorentz Force, Magnetic Field, PEM Water Electrolyzer

1. Introduction

The global energy demand is dependent on fossil fuels causing environmental problems due to the emission of harmful greenhouse gases (GHG) such as SO_x, C_nH_m, NO_x and CO_x. Thus, meeting the global energy demand from clean and renewable energy sources has become an international target with many countries committed to achieving it [1]. Hydrogen is an energy carrier that has higher specific energy density than any fossil fuel and no associated GHG emissions, which makes it an ideal candidate for storing renewable energy and replacing fossil fuels [2]. Among the various hydrogen energy production technologies, Proton Exchange Membrane Water Electrolyzer (PEMWE) has promising advantages due to its high efficiency and possibility to integrate with renewable energy sources such as solar, wind, wave, etc. [3-6]. The main barrier for PEMWEs commercialization is their high cost due to the use of expensive metallic electrocatalysts for oxygen evolution reaction (OER) and hydrogen evolution reaction (HER) at the anode and cathode respectively [7-11]. At the cathode, Pt catalyst is commonly used while metal oxides, namely; IrO_2 and RuO_2, are used at the anode providing high kinetic activity and durability [3, 12-15]. The literature indicates that IrO_2 is more durable than RuO_2 in an acidic environment however RuO_2 is more active for the OER. Thus, composite catalysts combining different noble metals or noble metals with non-noble metals have been explored [3, 16].

During operation, PEMWE suffer performance losses due to activation, ohmic and concentration overpotentials. The low activity of the electrocatalyst at the electrodes results in activation overpotentials. Ohmic losses are due to contact and internal resistances within the cell components. Finally, concentration overpotentials are the result of limitations in species mass transport from and to the active sites at the electrode. In PEMWE, bubbles are formed from the OER and HER reactions covering the electrical double layers and causing

concentration losses. The ability of the electrode to remove the formed bubbles is affected by the electrode surface, materials and the electrode geometry [17, 18].

During the OER in a PEMWE, the formed oxygen bubbles stick to the electrode surface causing a loss of active surface area and high mass transport overpotential [19]. Therefore, research were conducted on modifying the cell design to facilitate oxygen bubbles removal from the electrode surface and maintaining high performance especially at high current densities. The effect of external environments such as; microgravity, centrifugal force, ultrasonic and magnetic fields were investigated for aqueous water electrolyzers in order to achieve and maintain bubble free electrodes during the electrolyzer operation [20-24]. For example, Kiuchi et al. [23] investigated the galvanostatic water electrolysis under microgravity. They concluded that bubbles are attached to the electrode surface more than standard gravity conditions causing higher ohmic resistance inside the cell. In another study Lao et al. [25] investigated the centrifugal force effect on alkaline water electrolysis. They obtained almost three-fold increase in current density in centrifuged electrolysis conditions. Li et al. [26] investigated the presence of ultrasonic field on the water electrolyzers performance. They concluded that ultrasonic water electrolysis increases hydrogen production efficiency by 5-18%.

Among the physical fields studied in water electrolyzers, the use of a magnetic field is particularly promising due to magnetohydrodynamic (MHD) and magnetoaerodynamic (MAD) effects on the flow regions. In the liquid phase, MHD (Lorentz force) is more effective while in the gas phase MAD (Kelvin force) is more dominant. Applying an external magnetic field in perpendicular position to the current direction generates Lorentz Force, which ensures the convection of bubbles inside the cell [27]. Under the magnetic field, when current is parpendecular to the magnetic field, buoyancy force and Lorentz force push and separate the bubbles from the electrode surface. This improves mass transfer inside the cell. On the other hand, in the gas phase, due to the related magnetic properties of the gasses they can move in

different directions. It is commonly known that H_2 is diamagnetic gas but O_2 is a paramagnetic gas. Thanks to the different magnetic properties of O_2 and H_2 gases, the magnetic field provides a moving force and orientation. This provides enhanced proton transfer through the membrane and better gas seperation from the electrodes resulting in better mass transfer [27, 28].

Several studies in the literature reported an enhanced electrochemical cell performance under external magnetic field [29, 30]. The performance of different types of fuel cells under magnetic field was also investigated [31-33]. Furthermore, the effect of magnetic field on oxygen and hydrogen evolution reactions and the species transport in electrolyzers was studied [27, 28, 34]. Here, the effect of magnetic field in water electrolysis is very promising, especially in terms of the bubble separation from the electrode surface resulting in reduced mass transfer and ohmic losses and enhanced electrolyzer performance. We have recently demonstrated the positive effect of the application of an external magnetic field on the performance of PEMWEs [35].

Moreover, as oxygen is a paramagnetic molecule, the magnetic field can influence its direction [36]. Thus, it is possible to enhance its interaction with the electrode at the micro level by modifying the electrocatalyst through magnetizing the reaction interface or the material. Some studies investigated magnetically modified catalysts for electrochemical applications [37-39]. Li et al.[39] investigated the magnetic field effect on the oxygen evolution reaction in the magnetic Co_3O_4 semiconductor catalyst. They stated that the magnetic field increases the electrons spin energy and charge transfer kinetics in the catalyst. These factors not only improve the charge transport in the OER catalytic reaction substantially but also avoid the need for complex catalyst structural modification, morphological control, and material cladding. Moreover, they reported that the magnetic field provides easily controllable morphology and coatings by the help of its effect on the electrode surface. Okada et al.[37] studied Nd/Fe/B magnetic particles by directly applying it on the cathode catalyst layer of an PEM fuel cell to observe the effect on performance. The catalyst performance was studied ex-situ using a

rotating disk electrode and higher current density and limiting current were obtained with the magnetized catalyst. Recently, Shi et al. [38] studied a magnetically modified catalyst for PEM fuel cells. They used Pt-$Nd_2Fe_{14}B$ catalyst at the cathode and obtained four times increase in performance due to Kelvin force effect. Despite the promising results in PEM fuel cells, to the authors knowledge, there are no studies reported on the effect of applying magnetically modified catalyst in PEMWE.

In this study, the commonly used PEMWE anode catalyst (IrO_2) was modified with the magnetic Fe_3O_4 to investigate its effect on PEMWE performance. Thus, 90% IrO_2 - 10% Fe_3O_4 and 80%IrO_2 - 20%Fe_3O_4 samples were prepared and tested ex-situ in an electrochemical cell and in-situ in a PEMWE single cell. The results of non-magnetized and magnetized samples were compared to study the effect of the magnetic composite catalyst layer on the cell performance.

2. Experimental

2.1. Synthesis of IrO_2/Fe_3O_4 composites using Adam's Fusion Reaction

To prepare the catalyst in oxide structure, a modified Adam's Fusion method was used [40]. In this method, to obtain IrO_2, $IrCl_3.H_2O$ (99.9%, Aldrich) precursor was used. In addition, $IrCl_3.H_2O$ (99.9%, Aldrich) was used with $FeCl_2$ and $FeCl_3$ to obtain 80% IrO_2 - 20% Fe_3O_4, 90% IrO_2 - 10% Fe_3O_4, respectively. $FeCl_2.H_2O$ (98%, Aldrich) and $FeCl_3.H_2O$ (≥99.9%, Aldrich) were used to achieve 1/1.75 ratio of Fe^{2+}/Fe^{3+} and produce the IrO_2/ Fe_3O_4 composites [3, 40-42]. To prepare the composites, the relevant amount of $IrCl_3.H_2O$, $FeCl_2.H_2O$ and $FeCl_3.H_2O$ were dissolved in distilled water. Then 5 g of finely ground $NaNO_3$ (99.995%, Aldrich) was added to the solution and a homogeneous mixture was obtained . All mixtures were placed on a magnetic stirrer for about 1 hour to obtain homogeneous solutions.

Then, the mixtures were placed in a preheated oven at 80 ^{o}C to evoporate the water. The dried catalysts were placed in ceramic crucibles and sintered at 500 ^{o}C in air for one hour. The metal oxides obtained were then cleaned with distilled water and centrifuged. Finally, the metal oxide catalyst powders were dried in a vacuum oven at 80 ^{o}C. The prepared catalyst powders were then characterised with Scanning Electron Microscope (SEM) and Energy Dispersive X-Ray Analysis (SEM –EDX) under a 15kV electron beam using a table top SEM (Hitachi TM3030 plus) and X-Ray Powder Diffraction (XRD) (Bruker D2 benchtop, Co Tube) and X-ray Photoelectron Spectroscopy (XPS)(SPECS Inc.). Finally, Brunauer-Emmett-Teller (BET) measurement was conducted to obtain adsorption and desorption isotherms and find the catalyst surface area and average pore diameter. The test was conducted using a Micromeritics 3Flex BET surface area and microporosity masurement device.

Two composite catalyst compositions were investigated in this study, namely; 90% IrO_2 - 10% Fe_3O_4 and 80%IrO_2 - 20%Fe_3O_4. The composites were prepared by mixing catalyst inks with the relevant metal loading to obtain the targeted loading ratios. The indicated percent value in the composite name indicates molar percent in the compound.

2.2. Samples Preparation for Electrochemical Cell Testing

The electrochemical tests were conducted both in an electrochemical three-electrode wet cell, and in-situ in a singel polymer electrolyser cell. For the electrochemical wet cell, the catalyst powders were mixed in with the 5% Nafion® perfluorinated resin solution (5 wt. % in lower aliphatic alcohols and water, contains 15-20% water Aldrich) and ultrapure distilled water (Milli-Q®). The mixture was dispersed with an ultrasonic probe at 0.5 amplitute with 30 pulses for about 15 minutes to obtain a catalyst ink. A glassy carbon (GC) working electrodes (7.065 mm^2 surface area)were prepared with a total of 2.8 mg metals loading at different molar ratios. The catalyst was deposited on the clean GC electrodes via a micropipette, and then their

magnetized and non-magnetized performance was investigated. A three-electrode configuration was used in an electrochemical cell, with 0.5 M H_2SO_4 as the electolyte solution. The reference, counter and working electrodes were a saturated Ag/AgCl (206 mV potential shift compared to SHE), bright Pt mesh, and the GC electrode with the deposited catalyst respectively. A computer-controlled AMETEK ® Verstastat 3 Potentiostat was used to record linear-sweep voltammetry (LSV) and Chronoamperometry Analysis (CA). The LSV was obtained within the potential range of (0.0 -1.7 V vs. Ag/AgCl) at scan rate of 50mV s^{-1} and CA analysis are conducted for 40000 s at 1.5 V.

Moreover, PEMWE cell tests were conducted to observe the performane of the magnetized and non magnetized catalysts *in*-situ in a single cell PEMWE. Thus, a Membrane Electrode Assembly (MEA) with 5 cm^2 active area was used to validate the LSV results. Here, a Nafion 115 membrane was coated with 3 mg cm^{-2} anode catalyst using an airbrush and vacuum table to prepare catalyst coated membranes (CCM). Then, 0.4 mg cm^{-2} of Pt (20% Platinum on Vulcan XC 72-E-TEK) catalyst were coated on a Toray TGP-H-120-PTFE gas diffusion layer (GDL), respectively to obtain the cathode electrode. All components were assembled in an MEA by hot-pressing at 140 ^oC for 2 minutes. The MEA was then placed in a PEMWE single cell holder with a Pt coated Ti mesh as the anode GDL, and between two Ti current collectors. A gear pump was used to supply water to the PEMWE and the flow ratewas fixed at 100 ml min^{-1} for all experiments. Polarization curves (V-I) are obtained by an IviumStat XRi potentiostat in LSV mode with 10 mV s^{-1} scan rate between 0.0-2.5 V. Firstly, the non-magnetized samples were tested at 40 ^oC and 80 ^oC and then the samples were magnetized and tested at the same conditions.

2.3. Magnetization Method of the Samples

The modified GC electrodes and MEAs were magnitized by placing them in a specially designed holder within a magnetizer (Newport Instruments-Farnell). The magnetizer has an adjustable field strength and up to 2 T magnetic flux was used to modify the GC electrodes and MEAs (see Figure 1). The GC holder was made in-house, 3-D printed from PLA (non-conductive), with ports for the GC electrode and gaussmeter probe. All equipments for magnetization are designed for the saturation of the particles in relevant amount of magnetization.

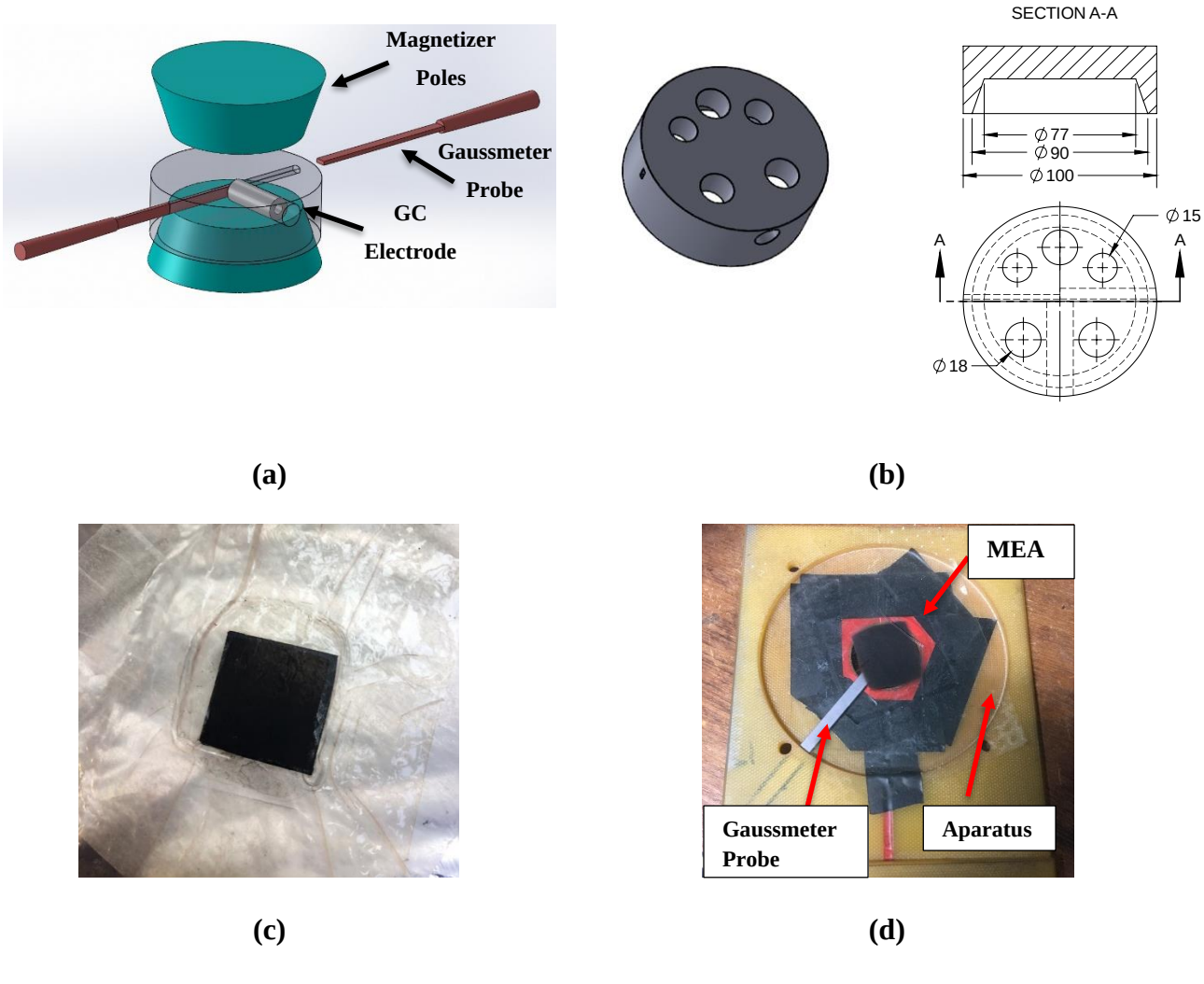

Figure 1. a) Magnetization apparatus design for the GC electrodes, b) 3D printed design , c) prepared MEA for magnetization and d) magnetization apparatus for MEAs.

To measure the particles magnetization level, horizontal and vertical gauss meter probe holes were introduced. In Figure 1.b, the top view and the cross-section of the equipment can be seen. Figure 1.c and 1.d present the MEA and its position on magnetization aparatus. The main advantage of the MEA magnetization apparatus is minimising the distance between the N-S poles. The generated magnetic flux density was measured using a LakeShore 455 DSP gaussmeter which has 10 μT sensitivity. The prepared MEAs were assembled and tested with the magnetized and non-magnetized conditions, respectively.

3. Results and Analysis

3. 1. Catalyst Materials Characterization

Firstly, the prepared metal oxide catalysts were physically characterisied via SEM-EDX, XRD, and BET surface area to determine their composition and structure before conducting the electrochemical tests. Fig. 2 shows the SEM-EDX images for 80% IrO_2 - 20% Fe_3O_4 and 90% IrO_2-10% Fe_3O_4 composite structures.

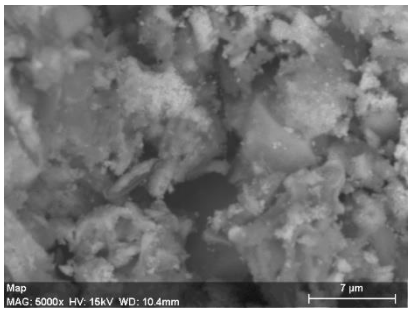

Element	wt. %	Atomic Percent
Iridium	54.07	14.55
Iron	27.33	25.32
Oxygen	18.60	60.13
Totals	100	100

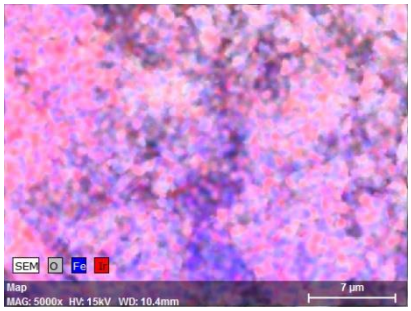

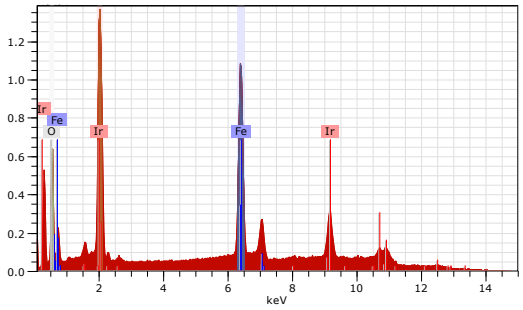

(a)

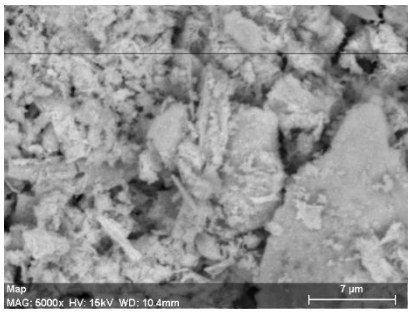

Element	wt. %	Atomic Percent
Iridium	68.61	16.31
Iron	2.94	2.40
Oxygen	28.45	81.28
Totals	100	100

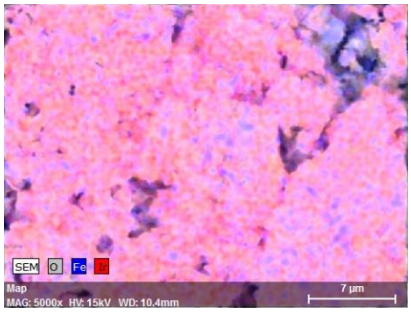

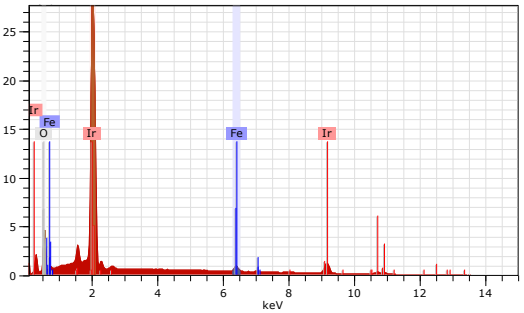

(b)

Figure 2. SEM EDX images for a) 80% IrO_2 - 20% Fe_3O_4 and b) 90% IrO_2 -10% Fe_3O_4 samples

The SEM and EDX images indicate that Ir, Fe and O are present in both samples and appear to be distributed homogeneously in the catalyst, and the presence of both Fe and Ir metal-oxides in the catalyst samples. Moreover, the EDX confirms that the amount of Fe is lower in 90%

IrO_2-10% Fe_3O_4 than in 80% IrO_2-20 %Fe_3O_4, as expected. Next, the XRD patterns were recorded for the two composites and can be seen in Figure 3.

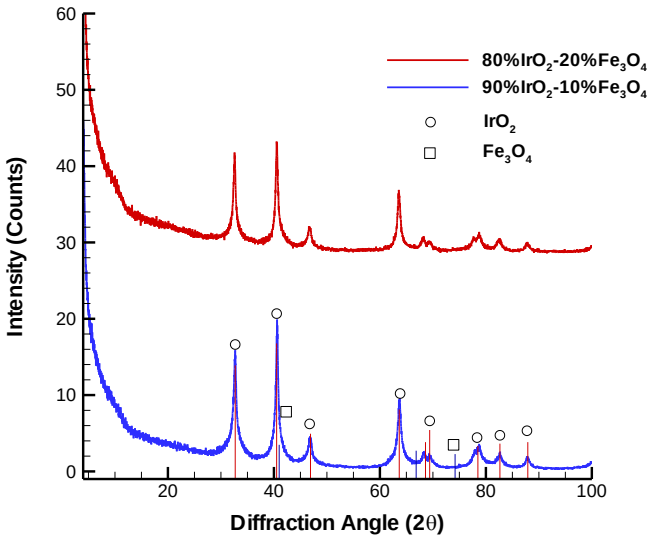

Figure 3. XRD patterns for 80%IrO_2-20%Fe_3O_4 and b) 90%IrO_2-10%Fe_3O_4 samples

The IrO_2 peaks in the XRD patterns can be seen clearly and fit with literature data [43]. The Fe_3O_4 peak regions [44] are very close to that for IrO_2 and due to the low amount in both samples the peaks cannot be observed clearly in the XRD pattern. However, there are slight shift in the peaks due to the different Fe_3O_4 and IrO_2 molar ratios. Therefore, XPS analysis was conducted to validate Fe_3O_4 structures as shown in Figure 4.

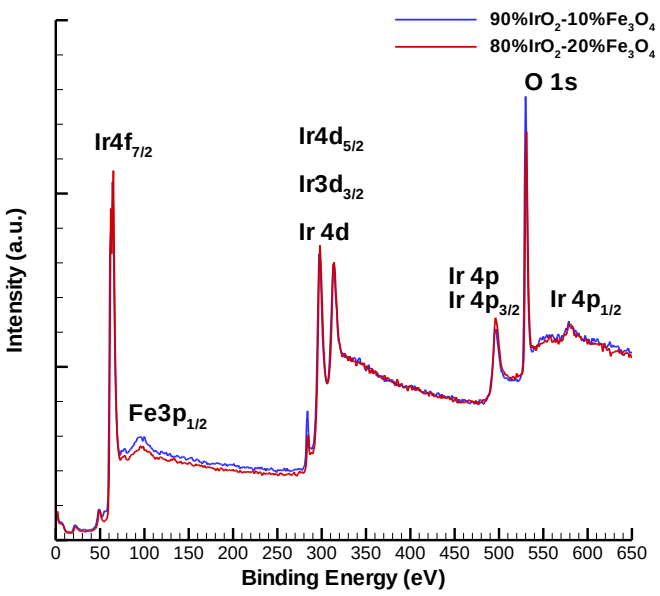

Figure 4. XPS analysis for different composite samples

As seen in Fig.4, Fe peak on $3p_{1/2}$ indicating the presence of Fe_3O_4 can be observed at 53.9 eV binding enegy [57, 58]. Moreover, on the 60.7, 300, 520 and 550 eV values, Ir peaks can be seen further confirming the presence of IrO_2 [59].

Finally, Table 1 provides a comparison of the BET results of the composite catalysts prepared in this work against the synthesised IrO_2. As can be seen in Table 1, BET surface area is highest in sythesized IrO_2 catalysts with 135.53 $m^2 g^{-1}$ value, and is reduced with the introduction of Fe_3O_4. The 90% IrO_2-10% Fe_3O_4 sample, has a surface area and pore diameter values very close to that measured for IrO_2, however, significant reduction in surface area and increase in porosity is shown for 80% IrO_2-20% Fe_3O_4 due to the reduced IrO_2 loading and increased Fe_3O_4 loading.

Table 1. BET surface area analysis of different samples and average pore diameters.

	BET Surface Area / $m^2 g^{-1}$	Average pore diameter / nm
Synthesized IrO_2	135.53	4.40
90% IrO_2-10% Fe_3O_4	131.3	4.6
80% IrO_2-20% Fe_3O_4	108.9	8.6

3.2. Magnetization of Electrode Materials

The GC and MEA samples were magnetized, and their magnetization level were measured, respectively. Table 2 shows the applied and measured magnetic flux density for the samples examined in the study.

Table 2. Applied and measured magnetic flux amount on the samples

Sample	Applied Magnetic Flux Amount with Magnetizer / T	Magnetization Time / min	Measured Magnetic Flux Amount on The Sample Surface / mT	Measured Magnetic Flux Difference on The Sample After Magnetization / mT
80%IrO_2-20%Fe_3O_4 on GC	1.6	3	0.192	0.072
90%IrO_2-10%Fe_3O_4 on GC	1.6	3	0.182	0.036
80%IrO_2-20%Fe_3O_4 on MEA	2	3	1.92	0.31
90%IrO_2-10%Fe_3O_4 on MEA	2	3	1.93	0.22

As seen in Table 2, The degree of magnetization is quite low with 0.072 and 0.036 mT for GC electrodes with the 80% IrO_2 - 20% Fe_3O_4 and 90% IrO_2 - 10% Fe_3O_4 catalysts, respectively. This is due to the low surface area of the GC (9.62 mm^2). Thus, a 5 cm^2 surface area of MEA was coated with the composite catalysts and magnetized to observe the effect of magnetic particles on a larger surface. After magnetization, the measured magnetic flux difference in the MEA samples were 0.31 and 0.22 mT for 80% IrO_2 - 20% Fe_3O_4 and 90% IrO_2 - 10% Fe_3O_4, respectively.

3.3. Analysis of electrochemical performances

To measure the electrochemical performance of the magnetized samples, LSV experiments were conducted. Firstly, LSV measurements of magnetized and non-magnezited particles were measured as shown in Figure 5.

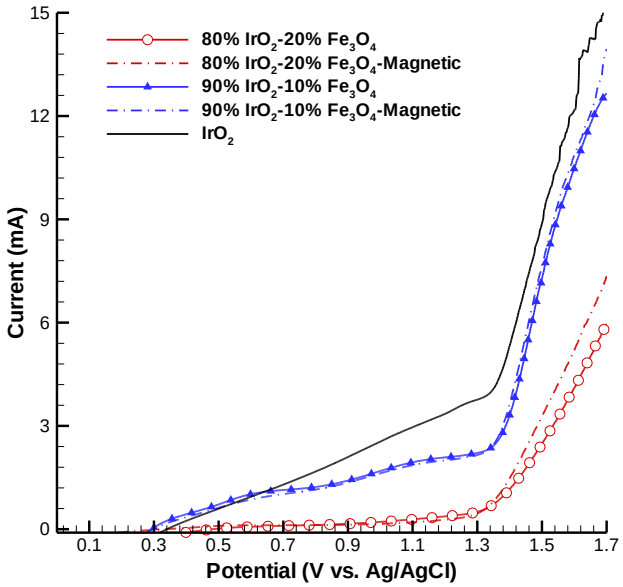

Figure 5. LSV curves for samples

With the addition of Fe_3O_4 to the IrO_2 for both samples (20% and 10% respectively), the performance of the catalyst decreases due to the lower catalytic activity of Fe_3O_4 and the reduction of IrO_2 loading. However, when these samples are magnetized at 1.6 T, the LSV curves are shifted closer towards the IrO_2 performance. The change in the LSV is mainly noticed at higher current density and therefore in the mass transport region. The improvement of current achieved at constant voltage for the 80%IrO_2-20%Fe_3O_4 sample after magnetisation is around 22% at 1.7 V.

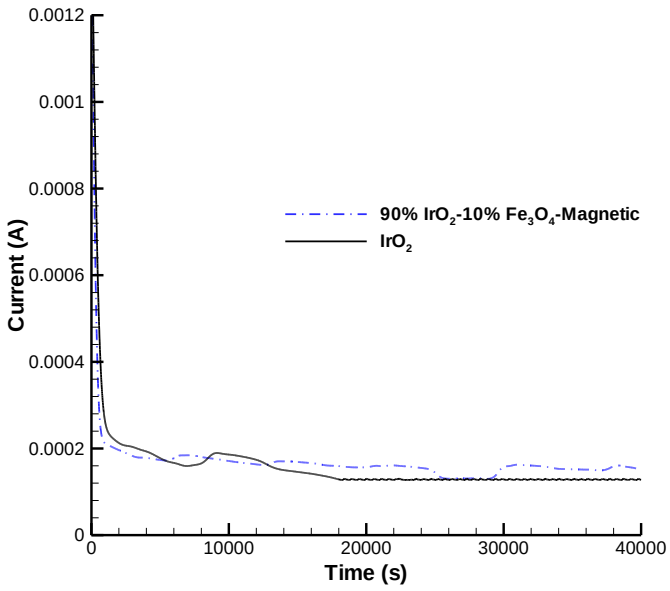

Figure 6. CA measurements for %90 IrO_2-%10 Fe_3O_4 and IrO_2

As seen in Figure 6, the CA measurements show the stability of Fe_3O_4 containing catalyst compared to pristine IrO_2 at 1.5 V. The detected increase in magnetic flux from the sample after magnetization is shown in Table 2, further confirming the presence and stability of magnetic effect in the catalyst layer in the MEA.

Figure 7 shows the maximum current density value obtained for each sample per mg of IrO_2. It is clear that the magnetized samples have a better performance at 1.7 V vs Ag/AgCl. Here, with 10 % Fe_3O_4 loading, the performance improvement from magnitisation is 9.5 %, and with 20 % Fe_3O_4 loading the performance improvement is around 22.2 %. Moreover, the 90% IrO_2-10% Fe_3O_4 showed relatively higher performance than that achieved by the prestine IrO_2 catalyst.

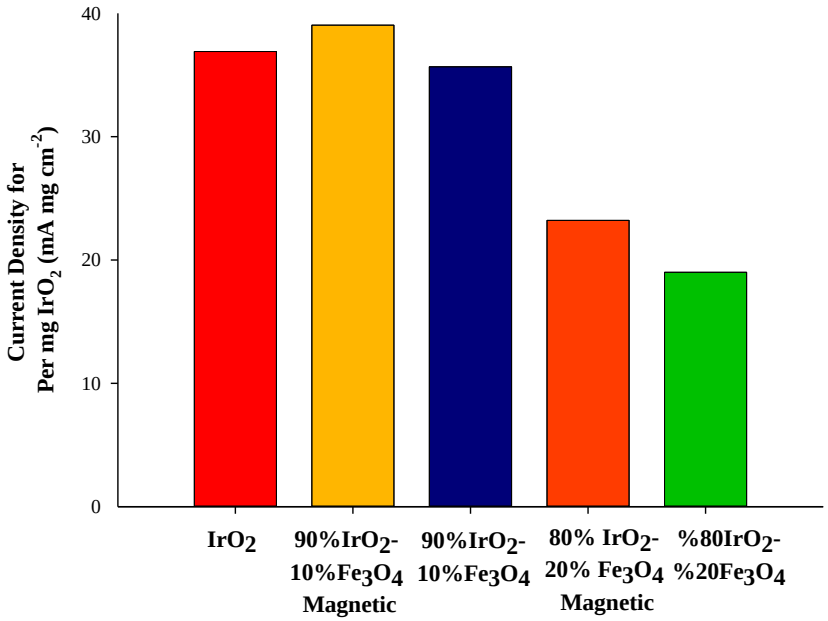

Figure 7. Current density value for per mg IrO_2 from the ex-situ LSV analysis

It can be concluded from these results that by magnetising the catalyst layer, higher current density can be achieved than that from a prestine IrO_2 catalyst layer. If such catalyst is used in a stack, they would decrease the amount of IrO_2 usage asnd as a result reduces the stack cost. These resuls are in line with expectations from the earlier review of the literature [38, 45]. Moreover, Tufa et al. [46] recently published the use of magnetic Ag@Fe3O4 magnetoplasmonic electrodes to observe the effect of Kelvin and Lorentz Force on electrochemical performance. They concluded that the magnetic flux applied on the electrode magnetized the Ag@Fe3O4 film. As a result, a highly nonuniform magnetic field, inducing Kelvin force near to the working electrode, is generated at the film surface. In their EIS analysis, the magnetic MagPlas3 film had bigger electron transfer and conductivity values. Moreover, when the samples were magnetized, the achieved current value increased from $3.5x10^{-5}$ A to $4x10^{-5}$ A. Thus, their reported results are in good agreement with the result achieved in this study.

Next, MEA testing was carried out to investigate if these promising ex-situ results could be replicated in a single-cell PEMWE. Figure 8 shows the results form the experiments carried out at 40 and 80 ºC.

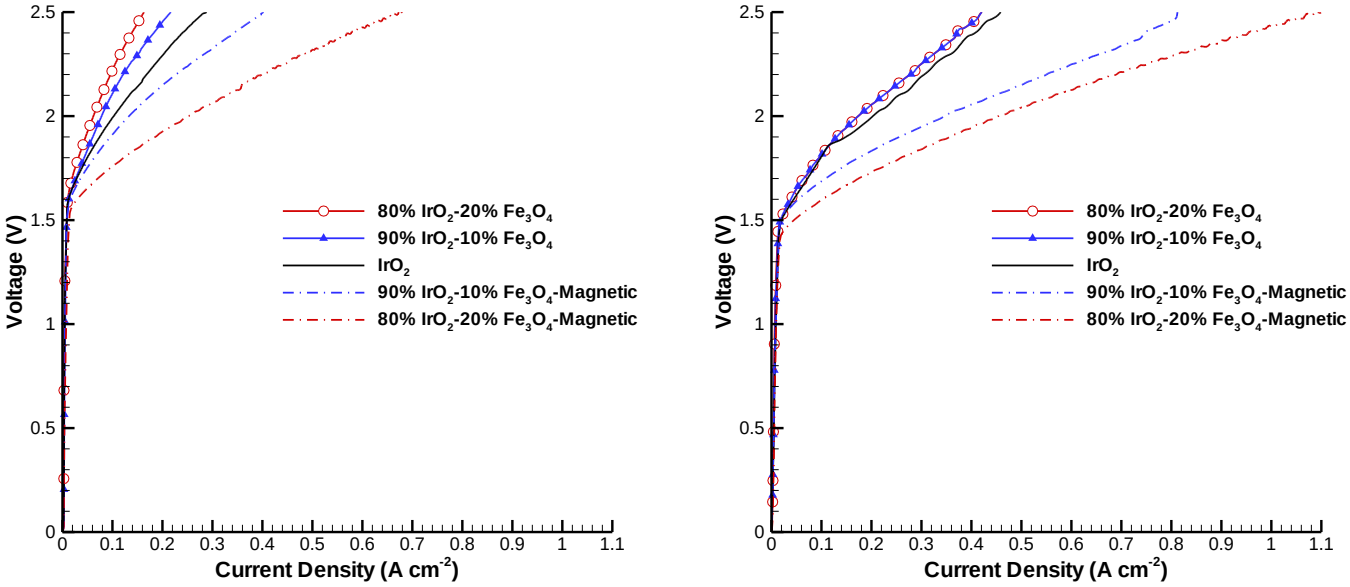

Figure 8. PEMWE Cell tests for composite samples a) at 40 ºC, b) at 80 ºC

According to Fig.8.a, IrO_2 had a better performance than the MEAs with catalyst containing non-magnetic 10% Fe_3O_4 and 20% Fe_3O_4 loading. By increasing the amount of Fe_3O_4 by 20%, the catalyst performance is decreased by around 20%. On the other hand, when the catalyst in the MEAs is magnetized in the magnetizer at 2 T, the samples containing 10% and 20% Fe_3O_4 display better performance than the prestine IrO_2. Particularly for the sample with 20% Fe_3O_4 loading where four times of the maximum current density for IrO_2 was achieved. With the 10% Fe_3O_4 sample, the improvement of performance is around 2.5 times higher than the non-magnetized sample. These results echo the behaviour seen in LSV measurements.

Moreover, as the conductivity and magnetic properties of Fe_3O_4 are reduced at higher temperature [47], the improvement in the electrolyser cell performance is more significant at

40 ˚C. The performance, as seen in Figure 9, shows the improvement in the performance in the mass transfer region and ohmic region of the polarization curve. Figure 8.b presents similar behaviour to that seen at 40 ºC, however the performance for the catalyst layer with 10 % and 20 % Fe_3O_4 loading is very close. At higher temperatures the activation polarization losses in the cell are lowered for all samples. When the samples with 10% and 20% Fe_3O_4 are magnetized, the current density value is increased significantly. The increase in the current density of the 20% Fe_3O_4 loading catalyst is twice of that of the non-magnetized sample. On the other hand, at 10% Fe_3O_4 loading, 1.5 times increase in the current density is achived with magnetisation. In Figure 9, at 80ºC, the maximum current density value obtained for each sample for per mg of IrO_2 can be seen.

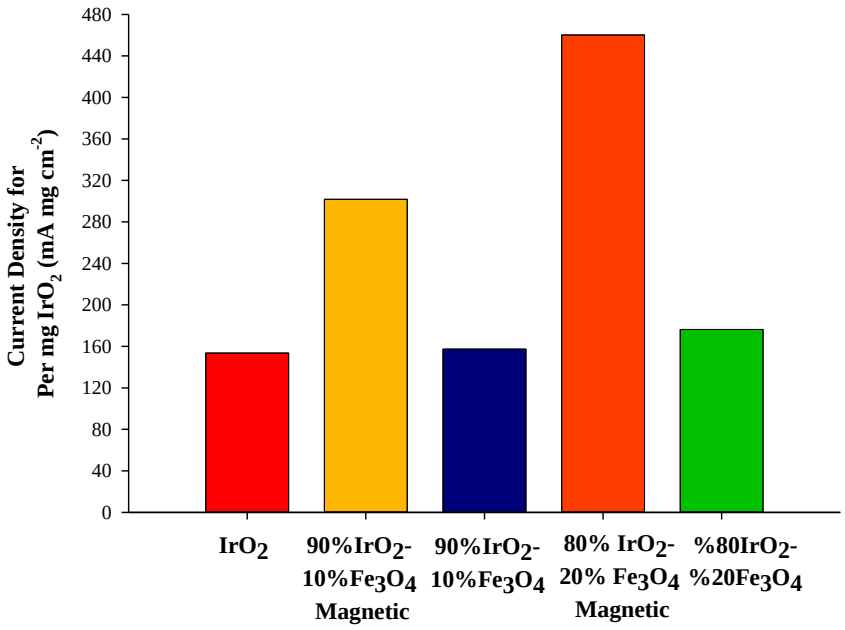

Figure 9. Current density value for per mg IrO_2 from polarization curve at 80 ºC

As seen in Figure 9, The addition of Fe_3O_4 before magnetization did not affect the maximum current density value per mg IrO_2. However, after magnetization, the 80% IrO_2 - 20% Fe_3O_4 and 90% IrO_2 - 10% Fe_3O_4 composite catalysts the maximum current density per mg IrO_2 is substantially increased. Moreover, the higher the magnetic Fe_3O_4 loading, the higher the

increase in current density. The catalyst layer with 80% IrO_2 - 20% Fe_3O_4 sample, the maximum current density per mg IrO_2 increased from 176.2 mA cm^{-2} to 460.2 mA cm^{-2} and for 90% IrO_2 - 10% Fe_3O_4 sample, the maximum current density per mg IrO_2 increased from 157.3 mA cm^{-2} to 301.8 mA cm^{-2}. It is possible to explain these effects on the gas phase phenomenon of magnetic forces. In liquid phase, the Lorentz force is dominant, but in the gas phase the Kelvin force affects the gas particles. O_2 which is paramagnetic gas, changes its direction through the magnetic flux direction. Thus, at the anode side, the ferromagnetic Fe_3O_4 particles enhance O_2 bubbles removal, accelerates their flow away from the catalyst active sites, and therefore increase the performance of the PEMWE.

4. Conclusion

Using Adam's fusion reaction, IrO_2 catalyst was synthesized successfully. Moreover, composite catalyst of IrO_2-Fe_3O_4 with different molar ratios was synthesized for the first time in the literature by a Modified Adam's Fusion Method. The synthesized catalysts were then coated on a GC and made into an MEA to study their *ex*-situ and *in*-situ electrochemical performance, respectively, and observe the catalyst magnetization effect. The results demonstrate, both in *ex*-situ and *in*-situ, an improvement in the composite catalyst electrochemical performance with magnetization. The magnetized catalyst layer achieved around 2.5- and 4-fold increase in the MEA maximum current density, at 10% and 20% Fe3O4 respectively, in comparison to the non-magnetized and pristine IrO_2 catalyst. This improvement was observed at both operating temperatures examined, namely, 40 ˚C and 80 ˚C.

It is important to highlight here that despite the decrease in the IrO_2 loading in the composite catalyst layer, significantly higher performance was achieved. In this study, the highest performing catalyst layer (80% IrO_2 - 20% Fe_3O_4) had 20% less IrO_2which was replaced by the abundant and cheap Fe_3O_4 (1 gr of IrO_2 is 300$ compared to 20$ for 1 gram). Therefore, a significant decrease in the cost of the catalyst layer and therefore the electrolyzer can be realized

by employing the magnetic composite catalysts developed in this study. In the future, other magnetic oxides like CrO_2, Fe_2O_3 will be studied to investigate their magnetization effect and corrosion performance as anode catalyst for PEMWE studies.

Acknowledgements

The authors would like to thank the Scientific Research Projects Unit of Erciyes University for funding and supporting the project under the contract number FKB-2019-9134. M.F.K. thanks The Scientific and Technological Research Council of Turkey (TÜBİTAK) "2211-C Priority Areas PhD Scholarship Program with the grant number 1649B031501867" and "2214-A International Research Fellowship Program for PhD Students with the grant number 1059B1416009042" for their scholarships. M.F.K also thanks University of Birmingham Fuel Cell Research Group for their collaboration during his PhD visiting research and Dr. Malik Degri in Magnetic Materials Research Group for their help in magnetizer device.

References

[1] Puthiyapura VK, Pasupathi S, Basu S, Wu X, Su H, Varagunapandiyan N, et al. RuxNb1−xO2 catalyst for the oxygen evolution reaction in proton exchange membrane water electrolysers. international journal of hydrogen energy. 2013;38:8605-16.

[2] Yilmaz C, Kanoglu M. Thermodynamic evaluation of geothermal energy powered hydrogen production by PEM water electrolysis. Energy. 2014;69:592-602.

[3] Felix C, Maiyalagan T, Pasupathi S, Bladergroen B, Linkov V. Synthesis and optimisation of IrO2 electrocatalysts by Adams fusion method for solid polymer electrolyte electrolysers. Micro and nanosystems. 2012;4:186-91.

[4] Santana MH, De Faria LA. Oxygen and chlorine evolution on RuO2+ TiO2+ CeO2+ Nb2O5 mixed oxide electrodes. Electrochimica acta. 2006;51:3578-85.

[5] Xu C, Ma L, Li J, Zhao W, Gan Z. Synthesis and characterization of novel high-performance composite electrocatalysts for the oxygen evolution in solid polymer electrolyte (SPE) water electrolysis. International Journal of Hydrogen Energy. 2012;37:2985-92.

[6] Yuzer B, Selcuk H, Chehade G, Demir M, Dincer I. Evaluation of hydrogen production via electrolysis with ion exchange membranes. Energy. 2020;190:116420.

[7] Balat M. Potential importance of hydrogen as a future solution to environmental and transportation problems. International journal of hydrogen energy. 2008;33:4013-29.

[8] Aho A, Antonietti M, Arndt S, Behrens M, Bill E, Brandner A, et al. Chemical energy storage: Walter de Gruyter; 2012.

[9] Huggins RA. Energy storage: Springer; 2010.

[10] Wu C, Li J, Zhang D, Yang B, Li L, Zhou T, et al. Electrospun transition/alkaline earth metal oxide composite nanofibers under mild condition for hydrogen evolution reaction. International Journal of Hydrogen Energy. 2016;41:13915-22.

[11] Elias L, Cao P, Hegde AC. Magnetoelectrodeposition of Ni–W alloy coatings for enhanced hydrogen evolution reaction. RSC Advances. 2016;6:111358-65.

[12] Marshall A, Børresen B, Hagen G, Tsypkin M, Tunold R. Hydrogen production by advanced proton exchange membrane (PEM) water electrolysers—Reduced energy consumption by improved electrocatalysis. Energy. 2007;32:431-6.

[13] Marshall AT, Sunde S, Tsypkin M, Tunold R. Performance of a PEM water electrolysis cell using IrxRuyTazO2 electrocatalysts for the oxygen evolution electrode. International Journal of Hydrogen Energy. 2007;32:2320-4.

[14] Song S, Zhang H, Ma X, Shao Z, Baker RT, Yi B. Electrochemical investigation of electrocatalysts for the oxygen evolution reaction in PEM water electrolyzers. international journal of hydrogen energy. 2008;33:4955-61.

[15] Cheng X, Shi Z, Glass N, Zhang L, Zhang J, Song D, et al. A review of PEM hydrogen fuel cell contamination: Impacts, mechanisms, and mitigation. Journal of Power Sources. 2007;165:739-56.

[16] Kaya M, Demir N. Numerical Investigation of PEM Water Electrolysis Performance for Different Oxygen Evolution Electrocatalysts. Fuel Cells. 2017;17:37-47.

[17] Vogt H. The role of single-phase free convection in mass transfer at gas evolving electrodes—I. Theoretical. Electrochimica acta. 1993;38:1421-6.

[18] Vogt H. The role of single-phase free convection in mass transfer at gas evolving electrodes—II. Experimental verification. Electrochimica acta. 1993;38:1427-31.

[19] KAYA MF. Investigation the PEM Water Electrolyzer Performance Under Magnetic Field and Development of Electrocatalyst (PEM Elektrolizörlerin Manyetik Alan Altındaki Çalışma Performansının İncelenmesi ve Katalizör Geliştirilmesi) [Doctoral Thesis]. Kayseri, Turkey: Erciyes University; 2018.

[20] Fernández D, Diao Z, Dunne P, Coey J. Influence of magnetic field on hydrogen reduction and co-reduction in the Cu/CuSO4 system. Electrochimica Acta. 2010;55:8664-72.

[21] Matsushima H, Iida T, Fukunaka Y. Gas bubble evolution on transparent electrode during water electrolysis in a magnetic field. Electrochimica Acta. 2013;100:261-4.

[22] Koza JA, Mühlenhoff S, Żabiński P, Nikrityuk PA, Eckert K, Uhlemann M, et al. Hydrogen evolution under the influence of a magnetic field. Electrochimica Acta. 2011;56:2665-75.

[23] Kiuchi D, Matsushima H, Fukunaka Y, Kuribayashi K. Ohmic resistance measurement of bubble froth layer in water electrolysis under microgravity. Journal of The Electrochemical Society. 2006;153:E138-E43.

[24] Wang M, Wang Z, Guo Z. Understanding of the intensified effect of super gravity on hydrogen evolution reaction. international journal of hydrogen energy. 2009;34:5311-7.

[25] Lao L, Ramshaw C, Yeung H. Process intensification: water electrolysis in a centrifugal acceleration field. Journal of applied electrochemistry. 2011;41:645.

[26] Wang C-C, Chen C-Y. Water electrolysis in the presence of an ultrasonic field. Electrochimica Acta. 2009;54:3877-83.

[27] Kaya MF, Demir N, Albawabiji MS, Taş M. Investigation of alkaline water electrolysis performance for different cost effective electrodes under magnetic field. International Journal of Hydrogen Energy. 2017;42:17583-92.

[28] Hinds G, Coey J, Lyons M. Influence of magnetic forces on electrochemical mass transport. Electrochemistry communications. 2001;3:215-8.

[29] Iida T, Matsushima H, Fukunaka Y. Water electrolysis under a magnetic field. Journal of the electrochemical society. 2007;154:E112-E5.

[30] Wang Y, Zhang B, Gong Z, Gao K, Ou Y, Zhang J. The effect of a static magnetic field on the hydrogen bonding in water using frictional experiments. Journal of Molecular Structure. 2013;1052:102-4.

[31] Yin Y, Huang G, Tong Y, Liu Y, Zhang L. Electricity production and electrochemical impedance modeling of microbial fuel cells under static magnetic field. Journal of Power Sources. 2013;237:58-63.

[32] Li W-W, Sheng G-P, Liu X-W, Cai P-J, Sun M, Xiao X, et al. Impact of a static magnetic field on the electricity production of Shewanella-inoculated microbial fuel cells. Biosensors and Bioelectronics. 2011;26:3987-92.

[33] Matsushima H, Iida T, Fukunaka Y, Bund A. PEMFC performance in a magnetic field. Fuel Cells. 2008;8:33-6.

[34] Devos O, Aaboubi O, Chopart J-P, Olivier A, Gabrielli C, Tribollet B. Is there a magnetic field effect on electrochemical kinetics? The Journal of Physical Chemistry A. 2000;104:1544-8.

[35] Kaya MF, Demir N, Rees NV, El-Kharouf A. Improving PEM water electrolyser's performance by magnetic field application. Applied Energy. 2020;264:114721.

[36] Cai J, Wang L, Wu P. Oxygen enrichment from air by using the interception effect of gradient magnetic field on oxygen molecules. Physics Letters A. 2007;362:105-8.

[37] Okada T, Wakayama NI, Wang L, Shingu H, Okano J-i, Ozawa T. The effect of magnetic field on the oxygen reduction reaction and its application in polymer electrolyte fuel cells. Electrochimica acta. 2003;48:531-9.

[38] Shi J, Xu H, Zhao H, Lu L, Wu X. Preparation of Nd2Fe14B/C magnetic powder and its application in proton exchange membrane fuel cells. Journal of Power Sources. 2014;252:189-99.

[39] Li Y, Zhang L, Peng J, Zhang W, Peng K. Magnetic field enhancing electrocatalysis of Co3O4/NF for oxygen evolution reaction. Journal of Power Sources. 2019;433:226704.

[40] Adams R, Shriner R. Platinum oxide as a catalyst in the reduction of organic compounds. III. Preparation and properties of the oxide of platinum obtained by the fusion of chloroplatinic acid with sodium nitrate1. Journal of the American Chemical Society. 1923;45:2171-9.

[41] Can K, Ozmen M, Ersoz M. Immobilization of albumin on aminosilane modified superparamagnetic magnetite nanoparticles and its characterization. Colloids and Surfaces B: Biointerfaces. 2009;71:154-9.

[42] Atacan K, Çakıroğlu B, Özacar M. Improvement of the stability and activity of immobilized trypsin on modified Fe3O4 magnetic nanoparticles for hydrolysis of bovine serum albumin and its application in the bovine milk. Food chemistry. 2016;212:460-8.

[43] Liu Y, Wang C, Lei Y, Liu F, Tian B, Wang J. Investigation of high-performance IrO2 electrocatalysts prepared by Adams method. International Journal of Hydrogen Energy. 2018;43:19460-7.

[44] Bertolucci E, Galletti AMR, Antonetti C, Marracci M, Tellini B, Piccinelli F, et al. Chemical and magnetic properties characterization of magnetic nanoparticles. 2015 IEEE International Instrumentation and Measurement Technology Conference (I2MTC) Proceedings: IEEE; 2015. p. 1492-6.

[45] Brijmohan SB, Shaw MT. Magnetic ion-exchange nanoparticles and their application in proton exchange membranes. Journal of Membrane Science. 2007;303:64-71.

[46] Tufa LT, Jeong K-J, Tran VT, Lee JJAam, interfaces. Magnetic-Field-Induced Electrochemical Performance of a Porous Magnetoplasmonic Ag@ Fe3O4 Nanoassembly. 2020;12:6598-606.

[47] Horng L, Chern G, Chen M, Kang P, Lee D. Magnetic anisotropic properties in Fe3O4 and CoFe2O4 ferrite epitaxy thin films. Journal of magnetism and magnetic materials. 2004;270:389-96.